




Contribution of various spin configurations to the radiationless decay of PsH

Iraj Masood , S. Zayad Munir , and M. Jamil Aslam 

Department of Physics, Quaid-i-Azam University, 45320 Islamabad, Pakistan

 (Received 5 December 2023; revised 16 February 2024; accepted 5 March 2024; published 25 March 2024)

Positronium hydride (PsH) is a weakly bound (molecular) state of two electrons (e^-), a positron (e^+), and a proton (p^+). Due to the $e^- - e^+$ annihilation, it decays to a number of processes, where the radiationless decay is one of the most important channels. In this decay process, the photons released from the $e^- - e^+$ annihilation are absorbed by the remaining e^- and p^+ in PsH, giving us $\text{PsH} \rightarrow e^- p^+$. For a particular spin (singlet) configuration of the constituents of PsH, the radiationless decay rate of PsH was determined by Aslam *et al.* [*Phys. Rev. A* **104**, 052803 (2021)]. In this work, we calculate the decay rate of $\text{PsH} \rightarrow e^- p^+$ by exercising all possible spin orientations of PsH and the final states e^- and p^+ . By summing all the contributions, we verify that the result is the same if we calculate it using the standard fermion spin-sum technique of quantum field theory.

DOI: [10.1103/PhysRevA.109.032820](https://doi.org/10.1103/PhysRevA.109.032820)

I. INTRODUCTION

In 1951, Ore first showed the existence of positronium hydride [1], which is a four-body system consisting of two electrons (e^-), a positron (e^+), and a proton (p^+) bound together weakly. That triggered a lot of theoretical interest, and the properties of PsH were studied [2–19] using the variational approach with different trial wave functions. The first successful experimental effort was made by Pareja *et al.* [20], in which they reported the existence of such a bound state within a condensed phase. However, the most convincing evidence of this compound was reported by Schrader *et al.* [21] in positron-methane collisions, and they estimated its binding energy as $E_b = -1.1 \pm 0.2 \text{ eV}$, which is in agreement with most of the theoretical predictions [4–6,9,11–13,17–19]. PsH is a special case of the Coulombic system that lies between H_2 and dipositronium molecules (Ps_2), and it is essentially a four-body system, in which the three light constituents ($2e^-$, e^+) cluster around the p^+ . In addition to the ground state of PsH, resonance states lying in the PsH scattering continuum have also been investigated (see, e.g., [22–24]).

The presence of e^- and e^+ makes PsH unstable against disassociation, causing it to decay into a number of final states. When e^+ meets e^- , they can form a spin-singlet or -triplet state, decaying into an even or odd number of photons. When the photons emitted through the annihilation are absorbed by the other constituents of PsH, the process is called radiationless decay; i.e., $\text{PsH} \rightarrow e^- p^+$. In Ref. [25], the decay rate is calculated for a particular spin orientation of the constituents of PsH, where the wave function of the two electrons is taken to be in a spin singlet ($\uparrow\downarrow - \downarrow\uparrow$)/ $\sqrt{2}$ and the positron has up spin (\uparrow). The proton is considered a static spinless source of the Coulomb interactions.

In this work, using two different methods, we will calculate the $\text{PsH} \rightarrow e^- p^+$ decay rate using all possible spin configurations of the initial- and final-state particles and see whether the results coincide. In the first method, we consider the following spin combinations for the constituents of PsH:

(1) Both the pair of electrons and ($e^+ p^+$) are in a spin-singlet state, and both are in a spin-triplet state.

(2) The two electrons are in a spin-singlet state, whereas ($e^+ p^+$) are in a spin-triplet state.

(3) The two electrons are in a spin-triplet state, and ($e^+ p^+$) are in a spin-singlet state.

Using these spin orientations, we will calculate the rate for each configuration and then sum them together according to their weighted averages. The second method is the standard textbook method, where we sum over the spins and calculate the traces using the Casimir trick. Finally, we will match the two results and see whether they agree with each other. This was already established for the radiationless decay of Ps_2 , which is also a four-body system [26].

This paper is organized as follows: In Sec. II we discuss the various possible Feynman diagrams contributing to this process. The rates for the particular spin orientations, as well as using the fermion spin-sum method for this decay, are discussed in detail there. Finally, in Sec. III, we conclude our findings. In the Appendixes, we tabulate the amplitudes for particular spin configurations and give the simplified form of the phase space for $\text{PsH} \rightarrow e^- p^+$.

II. RADIATIONLESS DECAY OF PsH

The decay rate of PsH proceeds due to the annihilation of e^- and e^+ , which is known as a two-particle coalescence probability. It corresponds to the expectation value of a two-particle delta function, i.e., δ_{-+} , where the subscripts denote the charges of the annihilating particles. Now if the photons emitted due to this annihilation are absorbed by the remaining e^- and p^+ in PsH, this results in a change in the energy momentum of e^- and p^+ . This is known as radiationless decay and corresponds to the coalescence probability of all four particles at one point, which is an expectation value of δ_{p+--} defined in Eq. (B7). In the weak binding limit, we can safely ignore the three momenta of initial-state particles compared to their masses in PsH; i.e., the four-momentum of the initial-state constituents for each electron and positron is ($m, \mathbf{0}$), and for the proton it is ($M, \mathbf{0}$).

Due to the antisymmetrization of electrons in the initial state, there are 12 possible Feynman diagrams which can be

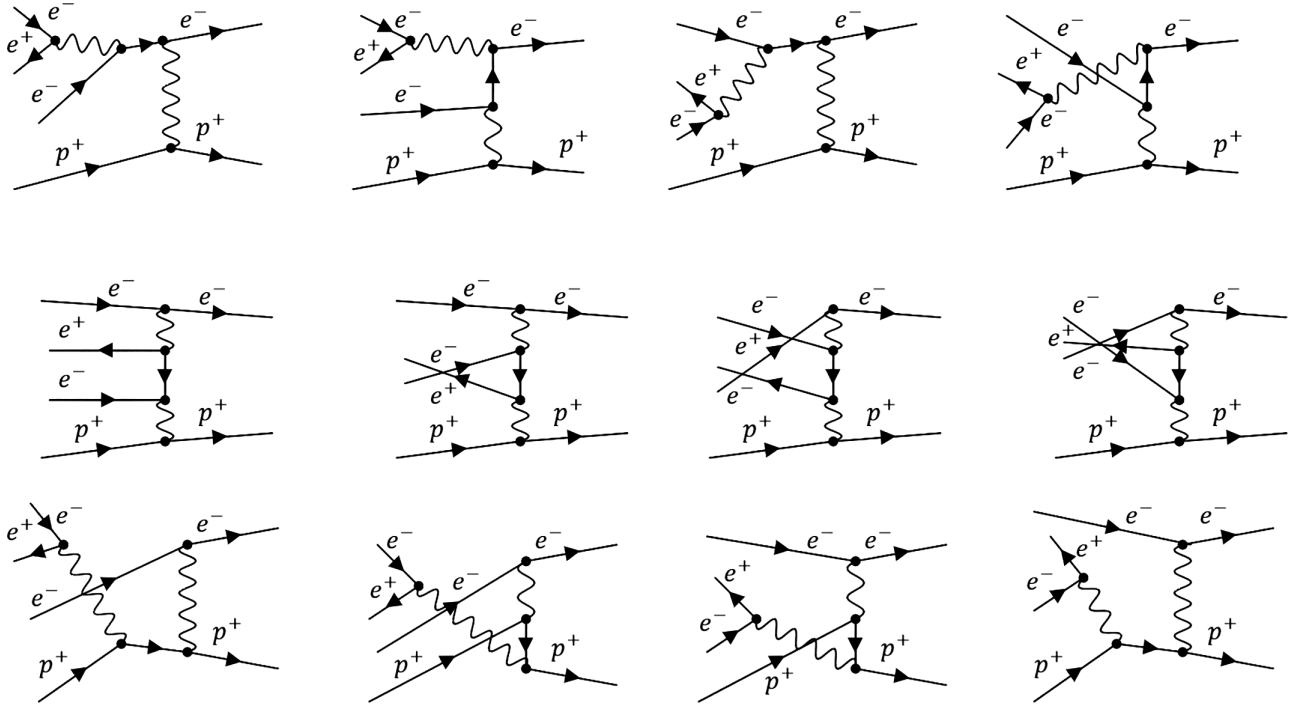


FIG. 1. The possible Feynman diagrams for $\text{PsH} \rightarrow e^- p^+$ at leading order (LO) in α . The diagrams in the first, second, and third rows are types A, B, and C, respectively.

generated using FEYNARTS [27]. They are drawn in Fig. 1. These topologies are divided into A-, B-, and C-type diagrams in Fig. 2. In A-type diagrams, for the nonzero value of the decay amplitude, the annihilating $e^- - e^+$ need to have the same spin (spin triplet). This resulting photon is absorbed by the remaining e^- in the initial state after bremsstrahlung. The bremsstrahlung photon is absorbed by the p^+ in PsH, leading to a change in its momentum. In B-type diagrams, the annihilation of $e^- - e^+$ is possible for the spin-singlet state, as it is annihilated into two photons. Both e^- and p^+ will absorb a photon in this case. The C-type diagrams are akin to the A-type ones, with the difference that in this case, it is the initial state p^+ that emits the photon (bremsstrahlung) and e^- in PsH that absorbs it. Here, we keep the mass of p^+ and calculate the results to the leading order in $\delta \equiv m/M$. Because the initial state has zero total momentum, we also assume that after absorbing the photons, the final states e^- and p^+ are moving back to back (say, along the z axis).

A. Specific spin orientations

In this section, we discuss the decay rate of $\text{PsH} \rightarrow e^- p^+$, employing a simplified spinor technique developed in [26] to calculate the decays of the positronium ion (Ps^-) and Ps_2 (see, e.g., [28] for a comprehensive review of these molecular states). The main idea of this technique is expressing the combination of Dirac spinors in terms of the γ matrices, which will help us to calculate the traces at an amplitude level.

Considering the proton as a static source of Coulomb interaction, a positron with spin up, and a pair of electrons in PsH in a spin-singlet state, the decay rate for $\text{PsH} \rightarrow e^- p^+$ was calculated in [25]. The corresponding result of the amplitude is

$$\mathcal{M} = -\frac{e^4}{8m^3}, \tag{1}$$

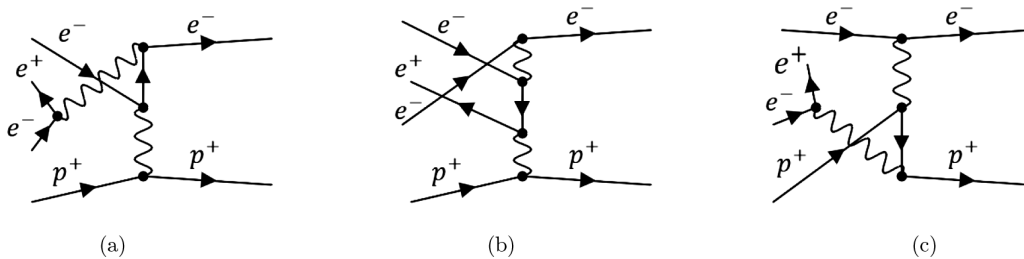


FIG. 2. A-, B-, and C-type Feynman diagrams for $\text{PsH} \rightarrow e^- p^+$.

TABLE I. The exact amplitude for all possible Feynman diagrams for various spin configurations of the constituents of PsH and the final states e^- and p^+ .

\mathcal{M}	$\mathcal{M}_{e_{\uparrow}^+ e_{\downarrow}^+ p_{\downarrow}^+}$	$\mathcal{M}_{e_{\downarrow}^+ e_{\uparrow}^+ p_{\uparrow}^+}$	$\mathcal{M}_{e_{\uparrow}^+ e_{\downarrow}^+ p_{\uparrow}^+}$	$\mathcal{M}_{e_{\downarrow}^+ e_{\uparrow}^+ p_{\downarrow}^+}$	$\mathcal{M}_{e_{\uparrow}^+ e_{\downarrow}^+ p_{\downarrow}^+}$	$\mathcal{M}_{e_{\downarrow}^+ e_{\uparrow}^+ p_{\uparrow}^+}$
\mathcal{M}_1	$\frac{\sqrt{2\delta+1}}{m^2(\delta+1)}$	$-\frac{\sqrt{2\delta+1}(3\delta+1)}{4m^2(\delta+1)^2}$	0	$-\frac{\sqrt{2\delta+1}(3\delta+1)}{4m^2(\delta+1)^2}$	$\frac{\sqrt{2\delta+1}(3\delta+1)}{4m^2(\delta+1)^2}$	$\frac{\sqrt{2\delta+1}}{2m^2(\delta+1)}$
\mathcal{M}_2	0	$\frac{\sqrt{2\delta+1}(3\delta+1)(\delta+3)}{4m^2(\delta+1)^3}$	$\frac{\sqrt{2\delta+1}(3\delta+1)}{m^2(\delta+1)^2}$	$\frac{\sqrt{2\delta+1}(3\delta+1)(\delta+3)}{4m^2(\delta+1)^3}$	$-\frac{\sqrt{2\delta+1}(3\delta+1)(\delta+3)}{4m^2(\delta+1)^3}$	$\frac{(\delta-1)\sqrt{2\delta+1}}{2m^2(\delta+1)^2}$
\mathcal{M}_3	$-\frac{\sqrt{2\delta+1}(3\delta+1)}{8m^2\delta}$	$\frac{\sqrt{2\delta+1}(3\delta+1)}{16m^2\delta}$	$-\frac{\sqrt{2\delta+1}(3\delta+1)}{8m^2\delta}$	$\frac{\sqrt{2\delta+1}(3\delta+1)}{16m^2\delta}$	$-\frac{\sqrt{2\delta+1}(3\delta+1)}{16m^2\delta}$	$-\frac{\sqrt{2\delta+1}}{4m^2}$
\mathcal{M}_4	$\frac{(\delta-1)\sqrt{2\delta+1}(3\delta+1)}{8m^2\delta(\delta+1)}$	$-\frac{\sqrt{2\delta+1}(3\delta+1)(\delta+3)}{16m^2\delta(\delta+1)}$	$\frac{(\delta-1)\sqrt{2\delta+1}(3\delta+1)}{8m^2\delta(\delta+1)}$	$-\frac{\sqrt{2\delta+1}(3\delta+1)(\delta+3)}{16m^2\delta(\delta+1)}$	$\frac{\sqrt{2\delta+1}(3\delta+1)(\delta+3)}{16m^2\delta(\delta+1)}$	$\frac{(\delta-1)\sqrt{2\delta+1}}{4m^2(\delta+1)}$
\mathcal{M}_5	$-\frac{\sqrt{2\delta+1}(3\delta+1)(\delta+3)}{4m^2(\delta+1)^3}$	0	$-\frac{\sqrt{2\delta+1}(3\delta+1)(\delta+3)}{4m^2(\delta+1)^3}$	$-\frac{\sqrt{2\delta+1}(3\delta+1)}{m^2(\delta+1)^2}$	$-\mathcal{M}_2$	$-\mathcal{M}_2$
\mathcal{M}_6	$\frac{\sqrt{2\delta+1}(3\delta+1)}{4m^2(\delta+1)^2}$	$-\frac{\sqrt{2\delta+1}}{m^2(\delta+1)}$	$\frac{\sqrt{2\delta+1}(3\delta+1)}{4m^2(\delta+1)^2}$	0	$-\mathcal{M}_1$	$-\mathcal{M}_1$
\mathcal{M}_7	$-\frac{\sqrt{2\delta+1}(3\delta+1)}{16m^2\delta}$	$\frac{\sqrt{2\delta+1}(3\delta+1)}{8m^2\delta}$	$-\frac{\sqrt{2\delta+1}(3\delta+1)}{16m^2\delta}$	$\frac{\sqrt{2\delta+1}(3\delta+1)}{8m^2\delta}$	$-\mathcal{M}_3$	$-\mathcal{M}_3$
\mathcal{M}_8	$\frac{\sqrt{2\delta+1}(3\delta+1)(\delta+3)}{16m^2\delta(\delta+1)}$	$-\frac{(\delta-1)\sqrt{2\delta+1}(3\delta+1)}{8m^2\delta(\delta+1)}$	$\frac{\sqrt{2\delta+1}(3\delta+1)(\delta+3)}{16m^2\delta(\delta+1)}$	$-\frac{(\delta-1)\sqrt{2\delta+1}(3\delta+1)}{8m^2\delta(\delta+1)}$	$-\mathcal{M}_4$	$-\mathcal{M}_4$
\mathcal{M}_9	$-\frac{(\delta-1)\sqrt{2\delta+1}(3\delta+1)^2}{16m^2\delta(\delta+1)^2}$	$\frac{\sqrt{2\delta+1}(3\delta+1)^2}{8m^2\delta(\delta+1)}$	$-\frac{(\delta-1)\sqrt{2\delta+1}(3\delta+1)^2}{16m^2\delta(\delta+1)^2}$	$\frac{\sqrt{2\delta+1}(3\delta+1)^2}{8m^2\delta(\delta+1)}$	$-\frac{(\delta-1)\sqrt{2\delta+1}(3\delta+1)^2}{16m^2\delta(\delta+1)^2}$	$\frac{\sqrt{2\delta+1}(3\delta+1)}{2m^2(\delta+1)}$
\mathcal{M}_{10}	$-\mathcal{M}_9$	$-\mathcal{M}_9$	$-\mathcal{M}_9$	$-\mathcal{M}_9$	$-\mathcal{M}_9$	0
\mathcal{M}_{11}	$\frac{\sqrt{2\delta+1}(3\delta+1)^2}{8m^2\delta(\delta+1)}$	$-\frac{(\delta-1)\sqrt{2\delta+1}(3\delta+1)^2}{16m^2\delta(\delta+1)^2}$	$\frac{\sqrt{2\delta+1}(3\delta+1)^2}{8m^2\delta(\delta+1)}$	$-\frac{(\delta-1)\sqrt{2\delta+1}(3\delta+1)^2}{16m^2\delta(\delta+1)^2}$	$\frac{(\delta-1)\sqrt{2\delta+1}(3\delta+1)^2}{16m^2\delta(\delta+1)^2}$	0
\mathcal{M}_{12}	$-\mathcal{M}_{11}$	$-\mathcal{M}_{11}$	$-\mathcal{M}_{11}$	$-\mathcal{M}_{11}$	$-\mathcal{M}_{11}$	$-\mathcal{M}_9$
\mathcal{M}_{tot}	$\frac{(\delta-1)\sqrt{2\delta+1}(5\delta^2+2\delta+1)}{8m^2\delta(\delta+1)^3}$	$-\frac{(\delta-1)\sqrt{2\delta+1}(5\delta^2+2\delta+1)}{8m^2\delta(\delta+1)^3}$	$\frac{\sqrt{2\delta+1}(3\delta+1)(7\delta^2+2\delta-1)}{8m^2\delta(\delta+1)^3}$	$-\frac{\sqrt{2\delta+1}(3\delta+1)(7\delta^2+2\delta-1)}{8m^2\delta(\delta+1)^3}$	0	0

and the resulting decay rate is

$$\Gamma(\text{PsH} \rightarrow e^- p^+) = \frac{\sqrt{2}\pi^3 \alpha^{13} m}{8} \langle \delta_{p+--} \rangle. \quad (2)$$

We know that in the case of $\text{Ps}_2 \rightarrow e^- e^+$ decay, the only nonzero decay rate is for spin-singlet pairs of electrons and positrons [29]. Here, we will see whether this is the case for $\text{PsH} \rightarrow e^- p^+$ decay too.

As a first step, unlike [25], we consider the spin of the p^+ in the initial and final states and calculate the rates for different spin orientations. In terms of these rates, the full decay rate of $\text{PsH} \rightarrow e^- p^+$ can be written as

$$\Gamma(\text{PsH} \rightarrow e^- p^+) = \frac{1}{16} (\Gamma^{(1,1)} + 3\Gamma^{(1,3)} + 3\Gamma^{(3,1)} + 9\Gamma^{(3,3)}), \quad (3)$$

where the superscripts represent the multiplicity of the spins of pair of electrons and the combined spin of positron and proton; for example, (1, 3) corresponds to the case when both electrons in PsH are in a spin-singlet state and p^+ and e^+ have the same spin (spin triplet). Furthermore, the decay rate associated with specific spin orientations is multiplied by the corresponding multiplicity factor. In this case, the factor $\frac{1}{16}$ is an overall normalization factor.

Singlet-singlet orientation. In this particular spin combination, using the technique developed in [26], the amplitudes for the 12 possible Feynman diagrams are calculated and given in Appendix B (see the first two columns of Table I). Expanding in leading powers of $\delta \equiv m/M$, the net amplitude in this case becomes

$$\mathcal{M}^{(1,1)} = \frac{\sqrt{2} M e^4}{8 m^3}. \quad (4)$$

It differs by a factor of $\sqrt{2}$ from the result (1) due to the spin of the proton, which does not occur Eq. (1). The decay rate of

$\text{PsH} \rightarrow e^- p^+$ can be written as

$$\begin{aligned} \Gamma(\text{PsH} \rightarrow e^- p^+) &= |\Psi(0, 0, 0, 0)|^2 \frac{1}{2} \int \frac{d^3 k_1}{(2\pi)^3 2|\mathbf{k}_1|} \frac{d^3 k_2}{(2\pi)^3 2|\mathbf{k}_2|} \\ &\times \frac{1}{\Pi_{\text{in}}(2E)} (2\pi)^4 \delta^4 \left(\sum_{i=1}^4 p_i - \sum_{j=1}^2 k_j \right) |\mathcal{M}|^2, \quad (5) \end{aligned}$$

where \mathcal{M} is the amplitude and $|\Psi(0, 0, 0, 0)|^2$ is the spatial wave function of PsH evaluated at the origin. $k_{1,2}$ represent the energies (momenta) of outgoing particles, which in terms of the masses of incoming particles are given in (A2). The energy E in $\Pi_{\text{in}}(2E)$ denotes the energy of individual constituents of PsH, which is equal to the mass of the respective particle. The denominator includes a factor of 2 to account for the indistinguishability of identical electrons in the initial state. We know that the wave function at the origin is related to the expectation value of the Dirac δ function, i.e., $|\Psi(0, 0, 0, 0)|^2 = \langle \delta_{p+--} \rangle a_0^{-9}$, where a_0 is the Bohr radius [25].

Using the result of phase space from Appendix A, the corresponding decay rate becomes

$$\Gamma^{(1,1)}(\text{PsH} \rightarrow e^- p^+) = \frac{\pi^3 \alpha^{13} m}{4\sqrt{2}} \langle \delta_{p+--} \rangle, \quad (6)$$

which agree with Eq. (2). Using $\alpha = 1/137$, $m = 0.511$ MeV, and $\delta_{p+--} = 1.8738 \times 10^{-4}$, which is presented in Table III of [19] for 4000 basis, we get

$$\Gamma^{(1,1)}(\text{PsH} \rightarrow e^- p^+) = 1.331 \times 10^{-10} \text{s}^{-1}. \quad (7)$$

Singlet-triplet orientation. In this case, the amplitudes of the individual diagrams and their sum are given in the third

and fourth columns of Table I (Appendix B). The corresponding sum of the amplitudes at leading order in m/M for all the diagrams gives

$$\mathcal{M}^{(1,3)} = \frac{\sqrt{2}Me^4}{8m^3}, \quad (8)$$

and the decay rate for this particular spin orientation becomes

$$\begin{aligned} \Gamma^{(1,3)}(\text{PsH} \rightarrow e^- p^+) &= \frac{\pi^3 \alpha^{13} m}{4\sqrt{2}} \langle \delta_{p+--} \rangle \\ &= 1.331 \times 10^{-10} \text{ s}^{-1}. \end{aligned} \quad (9)$$

Triplet-singlet and triplet-triplet orientations. In the limit of heavy protons, to leading order in m/M , the corresponding amplitudes add up to zero (fifth and sixth columns in Table I), i.e.,

$$\mathcal{M}^{(3,1)} = \mathcal{M}^{(3,3)} = 0, \quad (10)$$

and hence, we have

$$\Gamma^{(3,1)}(\text{PsH} \rightarrow e^- p^+) = \Gamma^{(3,3)}(\text{PsH} \rightarrow e^- p^+) = 0. \quad (11)$$

Assembling, Eqs. (6)–(11) in Eq. (3), the final result for the decay rate of PsH is

$$\Gamma(\text{PsH} \rightarrow e^- p^+) = \frac{\pi^3 \alpha^{13} m}{16\sqrt{2}} \langle \delta_{p+--} \rangle = 3.328 \times 10^{-11} \text{ s}^{-1}. \quad (12)$$

B. General spin configurations

The second method is based on the standard technique of particle physics, in which we write the amplitude, multiply it by its complex conjugate, and then average over the spins of initial-state particles and sum over the final ones. The same spinors sum up to give the trace, and this way of creating the trace is known as the Casimir trick, i.e.,

$$|\mathcal{M}|^2 = \frac{1}{16} \sum_{\text{all spins}} |\mathcal{M}|^2, \quad (13)$$

where the factor of $\frac{1}{16}$ ensures spin averaging over the initial-state particles.

Using FEYNARTS [27], one can generate all the possible Feynman diagrams and write the corresponding amplitudes. As there are 12 possible diagrams for this process, to find $|\mathcal{M}|^2$, we have to calculate 144 terms. To perform the fermion spin sum and to calculate the traces, we used the *Mathematica* package FEYNALC [30]. The corresponding $|\mathcal{M}|^2$ becomes

$$|\mathcal{M}|^2 = \frac{e^8 M^2}{2048 m^6}. \quad (14)$$

Using Eq. (14) together with Eq. (A4) and the kinematics in Eq. (5), the leading order in the m/M decay rate becomes

$$\Gamma(\text{PsH} \rightarrow e^- p^+) = \frac{\pi^3 \alpha^{13} m}{16\sqrt{2}} \langle \delta_{p+--} \rangle, \quad (15)$$

which is in agreement with the result presented in Eq. (12).

III. CONCLUSION

We have calculated the radiationless annihilation rate of PsH using two different techniques. In addition to the spin

orientation of the constituents of PsH considered in [25], we included all the other possibilities of the spins for the initial- and final-state particles. Using standard QED rules, we expressed the amplitudes in terms of the Dirac spinors, which, after we specify the spin orientation, can be expressed in terms of the traces of γ matrices. We found that if we include all possible spins and calculate the decay rate, the result is different from that in [25]. That was not the case for the similar decay of Ps₂, for which the rate does not change if we include all spin orientations [29]. With the second method, we drew the leading-order QED diagrams using automated computational tools, namely, FEYNARTS [27], and calculated the corresponding square of the amplitude using FEYNALC [30]. We found that all the diagrams are strongly correlated. Finally, we found that the results for the radiationless decay rate of PsH calculated using two different techniques are the same.

ACKNOWLEDGMENTS

M.J.A. would like to thank Prof. A. Czarnecki for providing an opportunity to work in his group during sabbatical leave from QAU and for introducing these problems. He further extends his thanks to M. Mubasher and W. Chen, who helped the authors at early stages of this work.

APPENDIX A: PHASE SPACE FOR PsH $\rightarrow e^- p^+$

The phase space for PsH $\rightarrow e^- p^+$ decay is calculated as

$$\begin{aligned} \int d\Pi_{\text{LIPS}} &= \int \frac{d^3 k_1}{(2\pi)^3 2|\mathbf{k}_1|} \frac{d^3 k_2}{(2\pi)^3 2|\mathbf{k}_2|} \\ &\quad \times (2\pi)^4 \delta^4 \left(\sum_{i=1}^4 p_i - \sum_{j=1}^2 k_j \right). \end{aligned} \quad (A1)$$

In the weak binding limit, we can ignore the momenta of the constituents of PsH compared to their masses; therefore, we can write $E = (m, 0, 0, 0)$ for each initial-state electron and positron and $E = (M, 0, 0, 0)$ for the proton. Hence, the total energy of the initial state is just $3m + M$. In order to conserve the three momenta, the final-state particles have to move back to back (say, along the z axis for convenience). Therefore, we can write the four-momenta k_1 and k_2 for p^+ and e^- , respectively, as

$$k_1 = (E_{k_1}, \mathbf{k}_1), \quad k_2 = (E_{k_2}, \mathbf{k}_2), \quad (A2)$$

where

$$\begin{aligned} E_{k_1} &= \frac{4m^2 + 3Mm + M^2}{3m + M}, \quad E_{k_2} = \frac{m(5m + 3M)}{(3m + M)}, \\ \mathbf{k}_1 &= -\mathbf{k}_2 = \left(0, 0, \frac{2m}{(3m + M)} \sqrt{2(m + M)(2m + M)} \right). \end{aligned}$$

Using these kinematics, Eq. (A1) simplifies to

$$\begin{aligned} \int d\Pi_{\text{LIPS}} &= \frac{\sqrt{m^2(2m^2 + 3mM + M^2)}}{\sqrt{2\pi}(3m + M)^2} \\ &= \frac{\sqrt{m^2 M^2 (2\delta^2 + 3\delta + 1)}}{\sqrt{2\pi} M^2 (3\delta + 1)^2}, \end{aligned} \quad (A3)$$

where $\delta = m/M$. To leading order in δ , we have

$$\int d\Pi_{\text{LIPS}} = \frac{1}{\sqrt{2\pi}}\delta. \quad (\text{A4})$$

APPENDIX B: AMPLITUDES FOR VARIOUS SPIN CONFIGURATIONS

The amplitudes for various spin combinations are given in Table I. To give an idea of how to calculate these amplitudes using the technique developed in [25], let us calculate it for the second diagram for the C-type ones shown in Fig. 2. Using the kinematics from Eq. (A2), the corresponding amplitude can be written as

$$\begin{aligned} \mathcal{M}_2 = & \frac{e^4(3m+M)^2}{64m^5(m+M)^3} [\bar{v}(p_2)\gamma^\mu u(p_1)][\bar{u}(k_2)\gamma_\alpha u(p_3)] \\ & \times \{\bar{u}(k_1)\gamma_\mu [(m-E_{k_2}+M)\gamma^0 + M + \mathbf{k}_2 \cdot \boldsymbol{\gamma}]\gamma^\alpha u(p_4)\}. \end{aligned} \quad (\text{B1})$$

Here, $p_{1,3}$ represent the momenta of electrons in the initial state, and p_2 and p_4 are the momenta of e^+ and p^+ , respectively. k_1 and k_2 correspond to the momenta of outgoing p^+ and e^- , respectively. For a particular spin orientation, we can switch the spinors in each bracket and form the trace, i.e.,

$$\begin{aligned} \mathcal{M}_2 = & \frac{e^4(3m+M)^2}{64m^5(m+M)^3} \text{Tr}[u_\uparrow(p_1)\bar{v}_\uparrow(p_2)\gamma^\mu] \\ & \times \text{Tr}[u_\downarrow(p_3)\bar{u}_\uparrow(k_2)\gamma_\alpha] \text{Tr}\{u_\uparrow(p_4)\bar{u}_\uparrow(k_1)\gamma_\mu\} \\ & \times [(m-E_{k_2}+M)\gamma^0 + M + \mathbf{k}_2 \cdot \boldsymbol{\gamma}]\gamma^\alpha. \end{aligned} \quad (\text{B2})$$

In our case, the initial-state particles are at rest; therefore, we can write

$$\begin{aligned} u_\uparrow = \sqrt{2m} \begin{pmatrix} 1 \\ 0 \\ 0 \\ 0 \end{pmatrix}, \quad u_\downarrow = \sqrt{2m} \begin{pmatrix} 0 \\ 1 \\ 0 \\ 0 \end{pmatrix}, \quad v_\uparrow = \sqrt{2m} \begin{pmatrix} 0 \\ 0 \\ 0 \\ -1 \end{pmatrix}, \\ v_\downarrow = \sqrt{2m} \begin{pmatrix} 0 \\ 0 \\ 1 \\ 0 \end{pmatrix}. \end{aligned} \quad (\text{B3})$$

Similarly, for the final-state proton we can write

$$\begin{aligned} u_\uparrow(k_1) = \sqrt{E_{k_1}+M} \begin{pmatrix} 1 \\ 0 \\ \frac{|\mathbf{k}_1|}{E_{k_1}+M} \\ 0 \end{pmatrix}, \\ u_\downarrow(k_1) = \sqrt{E_{k_1}+M} \begin{pmatrix} 0 \\ 1 \\ 0 \\ -\frac{|\mathbf{k}_1|}{E_{k_1}+M} \end{pmatrix}, \end{aligned} \quad (\text{B4})$$

and for the electron we have to replace M by m and E_{k_1} by E_{k_2} in Eq. (B4). The product of these spinors yields the 4×4 matrices, which can be expressed in terms of the γ matrices as

$$\begin{aligned} u_\uparrow(p_1)\bar{v}_\uparrow(p_2) &= -(2m)\frac{1+\gamma^0}{2}\frac{\gamma^1+i\gamma^2}{2}\gamma^0, \\ u_\downarrow(p_3)\bar{u}_\uparrow(k_2) &= \sqrt{2m(E_{k_2}+m)}\frac{\gamma^1-i\gamma^2}{2}\frac{\gamma^5-\gamma^3}{2} \\ & \times \left(1 + \frac{|\mathbf{k}_2|}{E_{k_2}+m}\gamma^5\right)\gamma^0, \\ u_\uparrow(p_4)\bar{u}_\uparrow(k_1) &= \sqrt{2m(E_{k_1}+M)}\frac{1+\gamma^0}{2}\frac{\gamma^5+\gamma^3}{2} \\ & \times \left(\gamma^5 + \frac{|\mathbf{k}_1|}{E_{k_1}+M}\right)\gamma^0. \end{aligned} \quad (\text{B5})$$

Inserting these combinations in Eq. (B2) and taking the trace give us the desired amplitude. Using a similar method for the other spin combinations, we can calculate the amplitudes given in Table I.

These are the free-state amplitudes, and they can be used to calculate the decay rate of a bound state as [31]

$$\begin{aligned} \Gamma(\text{PsH} \rightarrow e^- p^+) &= \frac{|\Psi(0,0,0,0)|^2}{2 \times 2M_T} \frac{1}{\Pi_{\text{in}}(2E)} \int \frac{d^3k_1}{(2\pi)^3 2|\mathbf{k}_1|} \\ & \times \frac{d^3k_2}{(2\pi)^3 2|\mathbf{k}_2|} (2\pi)^4 \delta^4 \left(\sum_{i=1}^4 p_i - \sum_{j=1}^2 k_j \right) \\ & \times |\mathcal{M}_f|^2, \end{aligned} \quad (\text{B6})$$

where $\mathcal{M}_f = \sqrt{2M_T}\mathcal{M}$, with M_T representing the total mass of the initial bound state. $|\Psi(0,0,0,0)|^2$ is the wave function of PsH at the origin. We can calculate it through the expectation value of the δ function, i.e.,

$$\langle \delta_{p+--} \rangle = \frac{\langle \Psi | \delta_{p+--} | \Psi \rangle}{\langle \Psi | \Psi \rangle}. \quad (\text{B7})$$

As PsH is a four-body system, if the positions of electrons are labeled 1 and 2 and those of e^+ and p^+ are labeled 3 and 4, respectively, the relative positions can be defined as

$$\vec{r}_{12} = \vec{r}_2 - \vec{r}_1, \quad \vec{r}_{13} = \vec{r}_3 - \vec{r}_1, \quad \vec{r}_{14} = \vec{r}_4 - \vec{r}_1. \quad (\text{B8})$$

Also, we can write

$$\vec{r}_{23} = \vec{r}_{13} - \vec{r}_{12}, \quad \vec{r}_{24} = \vec{r}_{14} - \vec{r}_{12}, \quad \vec{r}_{34} = \vec{r}_{14} - \vec{r}_{13}. \quad (\text{B9})$$

In the decay process we are discussing here, the electron and positron annihilate and produce photon(s), and they are later absorbed by the remaining constituents of PsH. Therefore, the four-particle coalescence probability can be calculated

as

$$\begin{aligned}
\langle \delta_{p+--} \rangle &\propto \langle \delta(\vec{r}_{12})\delta(\vec{r}_{23})\delta(\vec{r}_{34}) \rangle \\
&= \int d^3\vec{r}_{12}d^3\vec{r}_{13}d^3\vec{r}_{14}\delta(\vec{r}_{12})\delta(\vec{r}_{23})\delta(\vec{r}_{24})|\Psi(\vec{r}_{12}, \vec{r}_{13}, \vec{r}_{14}, \vec{r}_{23}, \vec{r}_{24}, \vec{r}_{34})|^2 \\
&\propto \int d^3\vec{r}_{12}d^3\vec{r}_{13}d^3\vec{r}_{14}\delta(\vec{r}_{12})\delta(\vec{r}_{23})\delta(\vec{r}_{14} - \vec{r}_{13})|\Psi(\vec{r}_{12}, \vec{r}_{13}, \vec{r}_{14}, \vec{r}_{23}, \vec{r}_{14} - \vec{r}_{12}, \vec{r}_{14} - \vec{r}_{13})|^2 \\
&\propto \int d^3\vec{r}_{12}d^3\vec{r}_{13}\delta(\vec{r}_{12})\delta(\vec{r}_{13} - \vec{r}_{12})|\Psi(\vec{r}_{12}, \vec{r}_{13}, \vec{r}_{13}, \vec{r}_{13} - \vec{r}_{12}, \vec{r}_{13} - \vec{r}_{12}, 0)|^2 \\
&\propto \int d^3\vec{r}_{12}\delta(\vec{r}_{12})|\Psi(\vec{r}_{12}, \vec{r}_{12}, \vec{r}_{12}, 0, 0, 0)|^2 \\
&\propto |\Psi(0, 0, 0, 0)|^2.
\end{aligned} \tag{B10}$$

For the particular choice of Ψ in the correlated Gaussian basis, its value is calculated in [19].

-
- [1] A. Ore, *Phys. Rev.* **83**, 665 (1951).
[2] S. M. Neamtan, G. Darewych, and G. Oczkowski, *Phys. Rev.* **126**, 193 (1962).
[3] V. I. Goldanskii, in *Positron Annihilation: Proceedings of the Conference Held at Wayne State University, July 27-29, 1965*, edited by A. T. Stewart and L. O. Roellig (Academic Press, Detroit, MI, 1967), pp. 183–258.
[4] C. F. Lebeda and D. M. Schrader, *Phys. Rev.* **178**, 24 (1969).
[5] P. B. Navin, D. M. Schrader, and C. F. Lebeda, *Appl. Phys.* **3**, 159 (1974).
[6] Y. K. Ho, *Phys. Rev. A* **17**, 1675 (1978).
[7] S. K. Houston and R. J. Drachman, *Phys. Rev. A* **7**, 819 (1973).
[8] B. A. P. Page and P. A. Fraser, *J. Phys. B* **7**, L389 (1974).
[9] P. B. Navin, D. M. Schrader, and C. F. Lebeda, *Phys. Rev. A* **9**, 2248 (1974).
[10] T. Yoshida and G. Miyako, *Phys. Rev. A* **54**, 4571 (1996).
[11] A. M. Frolov and V. H. Smith, *Phys. Rev. A* **56**, 2417 (1997).
[12] A. M. Frolov and V. H. Smith, *Phys. Rev. A* **55**, 2662 (1997).
[13] Y. Nagashima, T. Hyodo, K. Fujiwara, and A. Ichimura, *J. Phys. B* **31**, 329 (1998).
[14] Z.-C. Yan and Y. K. Ho, *Phys. Rev. A* **59**, 2697 (1999).
[15] A. M. Frolov, *Mol. Phys.* **120**, e2019337 (2022).
[16] J. A. Charry Martinez, M. Barborini, and A. Tkatchenko, *J. Chem. Theory Comput.* **18**, 2267 (2022).
[17] Z.-C. Yan and Y. K. Ho, *Phys. Rev. A* **60**, 5098 (1999).
[18] S. Bubin and L. Adamowicz, *Phys. Rev. A* **74**, 052502 (2006).
[19] S. Bubin and K. Varga, *Phys. Rev. A* **84**, 012509 (2011).
[20] R. Pareja, R. M. de la Cruz, M. A. Pedrosa, R. Gonzalez, and Y. Chen, *Phys. Rev. B* **41**, 6220 (1990).
[21] D. M. Schrader, F. M. Jacobsen, N.-P. Frandsen, and U. Mikkelsen, *Phys. Rev. Lett.* **69**, 57 (1992); E. L. Basor, C. A. Tracy, and H. Widom, *ibid.* **69**, 2880(E) (1992).
[22] J. DiRienzi and R. J. Drachman, *Phys. Rev. A* **76**, 032705 (2007).
[23] Z.-C. Yan and Y. K. Ho, *Phys. Rev. A* **84**, 034503 (2011).
[24] T. Yamashita, Y. Kino, E. Hiyama, S. Jonsell, and P. Froelich, *Few-Body Syst.* **62**, 81 (2021).
[25] M. J. Aslam, W. Chen, A. Czarnecki, M. Mubasher, and C. Stephens, *Phys. Rev. A* **107**, 062816 (2023).
[26] M. J. Aslam, W. Chen, A. Czarnecki, S. R. Mir, and M. Mubasher, *Phys. Rev. A* **104**, 052803 (2021).
[27] T. Hahn, *Comput. Phys. Commun.* **140**, 418 (2001).
[28] M. Emami-Razavi and J. W. Darewych, *Eur. Phys. J. D* **75**, 188 (2021).
[29] S. Z. Munir, M. Mubasher, and M. J. Aslam, *Europhys. Lett.* **141**, 44003 (2023).
[30] V. Shtabovenko, *J. Phys.: Conf. Ser.* **762**, 012064 (2016).
[31] M. E. Peskin and D. V. Schroeder, (Addison-Wesley, Reading, MA, 1995).